

# Nagaoka ferromagnetism in doped Hubbard models in optical lattices

Rhine Samajdar<sup>1,2</sup> and R. N. Bhatt<sup>1,3</sup>

<sup>1</sup>*Department of Physics, Princeton University, Princeton, NJ 08544, USA*

<sup>2</sup>*Princeton Center for Theoretical Science, Princeton University, Princeton, NJ 08544, USA*

<sup>3</sup>*Department of Electrical and Computer Engineering,  
Princeton University, Princeton, NJ 08544, USA*

(Dated: November 25, 2024)

The search for ferromagnetism in the Hubbard model has been a problem of outstanding interest since Nagaoka’s original proposal in 1966. Recent advances in quantum simulation have today enabled the study of tunable doped Hubbard models in ultracold atomic systems. Employing large-scale density-matrix renormalization group calculations, we establish the existence of high-spin ground states of the Hubbard model on finite-sized triangular lattices, analyze the microscopic mechanisms behind their origin, and investigate the interplay between ferromagnetism and other competing orders, such as stripes. These results explain—and shed new light on—the intriguing observations of ferromagnetic correlations in recent optical-lattice experiments. Additionally, we examine a generalized variant of the Hubbard model, wherein any second electron on a single lattice site is weakly bound compared to the first one, and demonstrate how this modification can lead to enhanced ferromagnetism, at intermediate length scales, on the nonfrustrated square lattice as well.

*Introduction.*—The Hubbard model is a paradigmatic model of modern condensed matter physics that is widely used to study a variety of strongly correlated systems [1]. It describes electrons hopping on a lattice with a tunneling amplitude  $t$  and interacting via an onsite potential  $U$ . Despite its seeming simplicity, this model harbors tremendously rich physics [2, 3] and is often believed to underlie a host of materials, including the high-temperature cuprate superconductors [4].

Over the last decade, ultracold atoms trapped in optical lattices have emerged as an exceptionally promising and versatile platform for realizing Hubbard models [5, 6]. Recently, a number of such cold-atom experiments [7–11] have demonstrated the existence of long-range antiferromagnetic order in two dimensions. Antiferromagnetism arises quite commonly in the Hubbard model, the magnetic excitations of which are described by a Heisenberg model of spins at half filling (one electron per site) [12] or, more generally, by a so-called  $t$ - $J$  model [13] in the doped system. In both cases, the electron-electron interactions give rise to a superexchange  $J \sim -t^2/U$  [14], which favors antialignment of spins.

Away from half filling, the kinetic term of the model can actually favor *ferromagnetism*, which is much rarer in the phase diagram. In 1966, Nagaoka [15] rigorously proved that for  $U/t = \infty$ , the ground state of the Hubbard model on a bipartite lattice with a single hole away from half filling is ferromagnetic [16]. For *finite*  $U/t$ , however, in the thermodynamic limit, the ground state is antiferromagnetic at half filling in all integer dimensions  $d > 1$  [17]. Since then, a number of studies have sought to determine if and when “Nagaoka ferromagnetism” is obtained for finite  $U/t$  [18–20] or practically relevant dopings [21–25] with varying degrees of success. In the absence of a conclusive answer, various routes towards *inducing* ferromagnetism in modified Hubbard models have

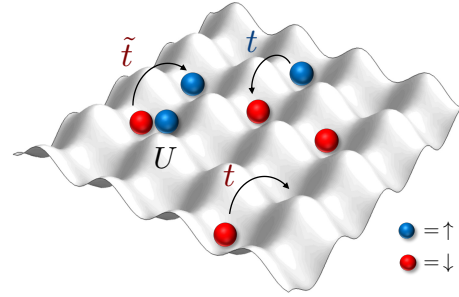


Figure 1. Schematic illustration of the Hubbard model and its extended variant, as described in Eqs. (1) and (2), respectively. Fermions hop on an optical lattice with an onsite repulsive interaction  $U$  and a tunneling amplitude  $t$ . We also consider a generalization of this model in which the tunneling matrix element is enhanced to  $\tilde{t}$  for a hopping process from a doubly occupied site to an already singly occupied site. In the limit  $\tilde{t} = t$ , the modified Hamiltonian reduces to that of the regular Hubbard model.

been explored, including the introduction of multiple orbitals, nearest-neighbor Coulomb repulsion, longer-range hoppings, or dispersionless (“flat”) bands in the spectrum [26–28].

In this work, we start by investigating the simple Hubbard model—without any of the aforementioned modifications—on a triangular lattice, which can be readily realized in today’s optical lattice setups. The Hamiltonian is given by

$$H = -t \sum_{\langle i,j \rangle, \sigma} \left( c_{i\sigma}^\dagger c_{j\sigma} + \text{h.c.} \right) + U \sum_i n_{i\uparrow} n_{i\downarrow}, \quad (1)$$

where  $n_{i,\sigma} \equiv c_{i,\sigma}^\dagger c_{i,\sigma}$  denotes the number operator on site  $i$ ,  $n_i = n_{i,\uparrow} + n_{i,\downarrow}$  is the total occupation of site  $i$ , and we only consider nearest-neighbor hopping. Studying the phase diagram of this model in the strong-correlation limit  $U \gg t$ , using large-scale density-matrix renormal-

ization group (DMRG) [29] calculations, we discover extended regions of ferromagnetic order in finite-sized strips. We characterize its intrinsic connection to geometric frustration and discuss its competition with other proximate orders, such as striped phases. Our results thus directly address the recent experiments by Xu *et al.* [30] observing ferromagnetism in a frustrated Fermi-Hubbard magnet and account for the origins thereof. Additionally, we demonstrate a route towards inducing ferromagnetism in the square lattice, which is not geometrically frustrated: this can be achieved in a setup where the second electron on any site of the lattice is much more weakly bound than the first and we examine the prospects for realizing such systems in optical lattices.

*Triangular lattice.*—Our search for elusive ferromagnetism begins with the triangular lattice motivated by Ref. 31, which established two conditions for the geometric constraints required to host Nagaoka ferromagnetism: the underlying lattice should have loops, and different paths of particles or holes around such loops should interfere constructively. On the unfrustrated square lattice, the shortest such path is a cluster of four sites, which leads to a hopping amplitude  $\sim t^4$ . However, it is the nonbipartite triangular lattice which exhibits the *shortest* possible loop length of three. Consequently, the loop-hopping amplitude is proportional to  $t^3$  and changes sign when  $t$  does (which is equivalent to exchanging electron and hole doping), so we expect to find ferromagnetism only for doping fractions  $\delta > 0$ .

We probe the ground states of the Hamiltonian (1) on two-dimensional cylinders of  $N$  sites, with dimensions  $L_x \times L_y$  (in units of the lattice spacing  $a$ ) and open (periodic) boundary conditions along the  $\hat{x}$  ( $\hat{y}$ ) direction [32]. Using DMRG with a bond dimension of up to  $\chi = 4800$ , we ensure the convergence of our results to a truncation error  $< 10^{-7}$  throughout. Earlier dynamical mean-field theory (DMFT) calculations on the Hubbard model found the region of ferromagnetism in parameter space to be maximized for an electron doping concentration of  $\delta = 0.5$  [33]. While DMFT is exact only in infinite dimensions, we use this filling fraction as a starting point for the Hubbard model (1) as well (note that this high-density regime is in distinction to Ref. 34, which illustrated the formation of *local* ferromagnetic polarons around a single doublon).

Figure 2 illustrates the ground states thus obtained for two representative values of  $U/t$ , at a doping fraction of  $\delta = 1/2$  above half filling. Here, the spin operator is defined as  $\mathbf{S}_i \equiv c_{i\alpha}^\dagger \boldsymbol{\sigma}_{\alpha\beta} c_{i\beta}$ . At  $U = 10t$ , one clearly observes a saturated ferromagnetic ground state, as evidenced by the uniform real-space spin-density profile plotted in Fig. 2(b) (for the sector with the largest  $S^z$  quantum number in the degenerate ground-state subspace). Interestingly, our calculations uncover a competing ground state with unidirectional charge and spin

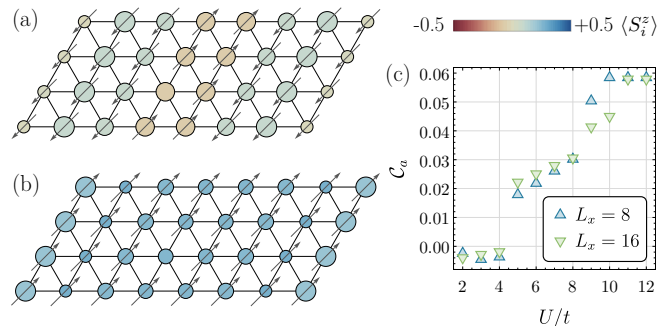


Figure 2. (a) Ground states of the Hubbard model (1) on a triangular lattice for (a)  $U/t=4$  and (b)  $U/t=10$ , exhibiting striped and ferromagnetic correlations, respectively. (c) The nearest-neighbor correlator  $C_a$ , plotted here for two width-4 cylinders of different lengths, shows the realization of the Nagaoka state for moderate  $U/t$ .

density modulations, for which the maximal allowed  $S^z$  quantum number is zero. An example of this inhomogeneous stripe-ordered state [35–37], which breaks translational and rotational symmetries, is displayed in Fig. 2(a) for  $U = 4t$ . Similar stripes have also been experimentally observed in certain square-lattice cuprates [38, 39]. In our case, the origin of the stripes can be understood from the competition between the domain walls favored by the antiferromagnetic exchange and the lack thereof preferred for kinetic delocalization. Consider a state with stripes of linear width  $\ell$ . Relative to the uniform ferromagnet, the increase in the electrons’ kinetic energy will be  $E_K \sim (\delta N) \tilde{t}/(\ell L_y)$  while the decrease in interaction energy due to the exchange across the domain walls is  $E_J \sim -JN/\ell$ . The contest between these two energy scales decides between ferromagnetic and stripe orders, with the former eventually prevailing at large enough  $U/t$  (as  $J \sim -t^2/U$ ).

Having established the existence of the Nagaoka state, we now turn to characterizing its extent and stability. A useful metric to quantify the the ferromagnetic order is the (normalized) average two-point correlation function  $C_d = \sum_{\langle i,j \rangle, \|\mathbf{r}_i - \mathbf{r}_j\|=d} \langle \mathbf{S}_i \cdot \mathbf{S}_j \rangle / \mathcal{N}_d$ , where the sum runs over  $\mathcal{N}_d$  unordered pairs of sites  $\langle i, j \rangle$  separated by a distance  $d$ . In particular, Fig. 2(c) shows the nearest-neighbor correlator  $C_a$  as a function of  $U/t$  for two different system sizes. To eliminate the possibility of strong finite-size effects, we consider two different cylinders with one being double the length of the other (results on wider cylinders are documented in the Supplemental Material [SM] [40]). In both cases, we see that the nearest-neighbor radial correlator  $C_a$  attains its maximum possible value by  $U/t \simeq 11$  although the onset of ferromagnetic correlations can already be seen for much lower  $U/t \sim 6$ . We emphasize that this observed ferromagnetism is truly a many-body phenomenon of the Nagaoka type, as opposed to Stoner ferromagnetism, which occurs whenever the (single-particle) density of states at the Fermi en-

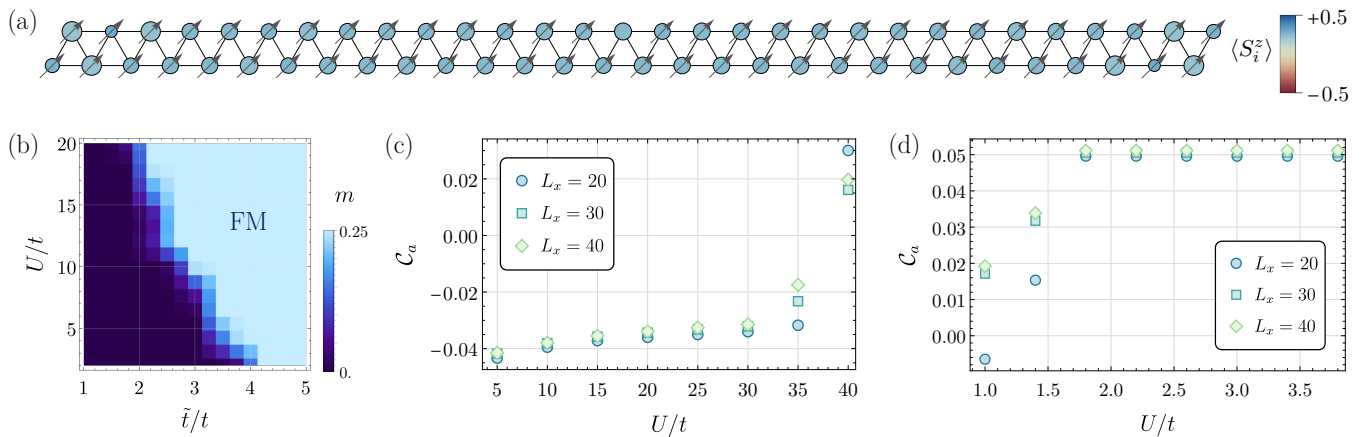


Figure 3. (a) Ground state obtained on a triangular two-leg ladder for  $\tilde{t}/t=4$ ,  $U=0.5\tilde{t}$  (drawn using the same conventions as in Fig. 2), displaying macroscopic long-ranged ferromagnetic correlations. (b) Phase diagram of a  $L_x=20$  ladder, as chalked out by the net magnetization,  $m$ , showing the extent of the Nagaoka state (FM). (c,d) The nearest-neighbor correlator  $C_a$  for ladders of three different lengths, demonstrating the development of ferromagnetism as a function of  $U/t$  along the cuts (c)  $\tilde{t}/t=1$  (the Hubbard limit) and (d)  $\tilde{t}/t=4$ . All calculations presented here are for an electron doping concentration of  $\delta=0.5$ .

ergy  $D(E_F) > 1/U$  and should thus set in for infinitesimal  $U/t > 0$  (as  $D(E_F)$  is singular at this filling; see below).

*Two-leg triangular ladders.*—While our results in the previous section manifest the presence of the Nagaoka state, classically, one might suspect this to be an effect of the geometric frustration, which is deleterious to competing antiferromagnetic orders and leads to their suppression. Such a reasoning, however, may break down due to subtle quantum effects; for example, antiferromagnetism can actually be *enhanced* on the triangular lattice by a single hole [41]. Instead, Nagaoka ferromagnetism on the triangular lattice can be better understood as a consequence of geometrical frustration of the kinetic energy—a strictly quantum-mechanical effect stemming from constructive interference between different paths of a doublon propagating in a spin-polarized background [41]. A quantitative measure of such kinetic energy frustration is given by  $f \equiv W/(2z|t|)$ , where  $W$  is the bandwidth and  $z$  is the coordination number [42], with smaller ratios indicating stronger frustration. The kinetic frustration of even a single triangular cluster results in lowering  $f$  below the unfrustrated value of  $f=1$  for the square lattice [33]. For the triangular-lattice Hubbard model, the noninteracting problem has a bandwidth of  $9t$  with  $z=6$ , wherefore  $f=0.75$ . The associated  $D(E)$  can be computed analytically in terms of a complete elliptic integral of the first kind and exhibits a van Hove singularity at  $E=-2t$ , corresponding to a density of 1.5 electrons per site. Our earlier choice of  $\delta=0.5$  thus maximizes  $D(E_F)$ : a large density of states at the Fermi level lowers the kinetic cost of filling additional single-particle electronic states, thereby enabling the large  $U$  (that favors spin alignment) to dominate [43–45].

In order to probe the dependence of ferromagnetism on  $f$ , we now consider a different geometry, namely, a two-leg triangular ladder, which has a reduced coordina-

tion number compared to the full lattice. In consistency with the intuition developed above, here, we do not find a ferromagnetic ground state for up to  $U/t=20$ . It is therefore only natural to ask if there are conditions under which ferromagnetism can occur for moderate values of  $U/t$  as well.

To answer this question affirmatively, we turn to a generalized Hubbard model—inspired by studies of hydrogenic donors in semiconductors [46–48]—in which the second electron on any site of the lattice is much more weakly bound than the first [49–51]. The Hamiltonian is [46, 47]

$$H = - \sum_{\langle i,j \rangle, \sigma} \left( t(n_i, n_j) c_{i\sigma}^\dagger c_{j\sigma} + \text{h.c.} \right) + U \sum_i n_{i\uparrow} n_{i\downarrow}; \quad (2)$$

the occupation-dependent nearest-neighbor hopping is given by  $t(n_i, n_j) = \tilde{t}$  if  $n_i=1, n_j=2$  and  $t(n_i, n_j) = t$  otherwise. This enhanced hopping (for electron-doped systems) favors the formation of a locally ferromagnetic configuration of spins around the charge, thus yielding a polaronic type of ferromagnetism in the large- $U/t$  limit [52].

Figure 3(a) sketches the ground state of this Hamiltonian on a 30-site-long two-leg ladder for  $\tilde{t}/t=4$ ,  $U=0.5\tilde{t}$ . Even for this rather small value of  $U/t$ , we unambiguously observe large-scale ferromagnetic order across our entire finite-sized system, characterized by a saturated net magnetization of  $m=0.25$  with a standard deviation of 0.015. Motivated by this finding, we systematically explore the dependence of ferromagnetism on the Hamiltonian’s parameters by constructing a phase diagram based on the magnetization  $m$  [Fig. 3(b)]. We see that increasing  $\tilde{t}/t$  results in a dramatic reduction in the minimal  $U/t$  needed for the development of ferromagnetic order. We examine the robustness of this behavior by inspecting the two-point correlator  $C_a$  along two cuts through

this phase diagram, for three ladders of varying lengths. For the Hubbard limit  $\tilde{t}/t=1$  [Fig. 3(c)], we find that the correlations in the ground state (which is believed to be a Curie-Weiss metal for low  $U/t$  [33]) remain negative till  $U/t \sim 40$  and turn weakly ferromagnetic thereafter. On the contrary, for  $\tilde{t}/t = 4$  [Fig. 3(d)], this transition occurs for a nearly twentyfold smaller  $U/t$ , irrespective of system size.

Lastly, we note that decreasing (increasing)  $\tilde{t}/t$  increases (decreases) the minimum  $U/t$  required for a fully polarized ground state. For instance, in stark contrast to Fig. 3(a), we do not detect any Nagaoka ferromagnet up to  $U/t=50$  for  $\tilde{t}/t=2$  (or, as seen earlier, for the Hubbard model at  $\tilde{t}/t=1$ ) on the same two-leg cylinders. This is because ferromagnetism is driven by the relative kinetic energy gain of a delocalized electron in a background of aligned spins vis-à-vis the background being in an antiferromagnetic or random configuration, and this gain is reduced by a smaller hopping amplitude.

*Square lattice.*—Our observation of Nagaoka ferromagnetism on the nonbipartite triangular lattice, which inately lacks electron-hole symmetry, raises the question of whether similar electron-hole asymmetry *induced* by setting  $\tilde{t} \neq t$  can aid the formation of ferromagnetic states or domains on even (bipartite) square arrays.

At half filling, the ground state of the square-lattice Hubbard model is known to be a Mott insulator with antiferromagnetic Néel order for all values of  $U/t > 0$  due to the perfect nesting of the noninteracting Fermi surface. As the doping (either electron or hole) is increased, one expects a transition to a ferromagnetic ground state for sufficiently large  $U/t$ . Exact diagonalization calculations on small clusters [46, 47] have previously found that high-spin ground states are obtained at much lower values of  $U/t$  for electron doping than for hole doping. Therefore, we consider the electron-doped case hereafter (focusing on the optimal doping fraction of  $\delta=1/12$  identified in Ref. 52) and without loss of generality, set  $\tilde{t}/t = 4$ .

At low  $U/t$ , we once again find a state with striplike correlations in the spin density (i.e., with *local* ferromagnetic order), as exemplified by Fig. 4(a) for a  $12 \times 4$  cylinder at  $U=6\tilde{t}$ . The long-ranged correlations in this state are reflected in the static structure factor  $\mathcal{S}(\mathbf{q}) = \sum_{i,j} \langle \mathbf{S}_i \cdot \mathbf{S}_j \rangle \exp[i\mathbf{q} \cdot (\mathbf{r}_i - \mathbf{r}_j)]/N$ , shown in Fig. 4(c).  $\mathcal{S}(\mathbf{q})$  has prominent peaks at  $(\pm\pi/3, 0)$  indicating a period-6 modulation of the spin density along the nonperiodic direction, which accompanies a period-3 modulation of the charge density. Across a wide range of  $L_x$ , we find that the stripes are filled and commensurate with the doping, accommodating exactly one excess electron per unit cell of 12 sites. Remarkably, at larger  $U=9\tilde{t}$ , we see clear evidence of a *global* ferromagnetic ground state, as displayed in Figs. 4(b) and (d) in real and Fourier space, respectively; in this fully polarized state, the structure factor only exhibits a single peak at  $\mathbf{q}=0$  in the Brillouin zone.

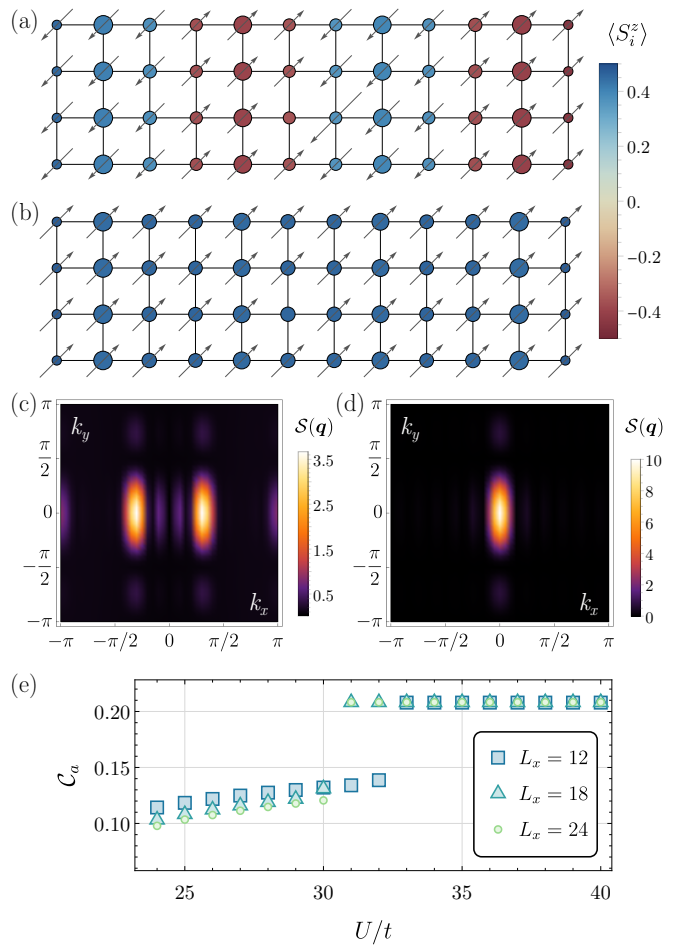


Figure 4. Ground states of the extended Hubbard model (2) at  $\tilde{t}/t=4$  for (a)  $U=6\tilde{t}$  and (b)  $U=9\tilde{t}$  on the square lattice. The color of each circle conveys the onsite magnetization  $\langle S_i^z \rangle$  while its diameter is proportional to the charge density  $\langle n_i \rangle$ . The length of the arrows is proportional to the amplitude of the spin correlation  $\langle \mathbf{S}_0 \cdot \mathbf{S}_i \rangle$  with respect to the central site, indexed 0 (arrow-free). The directions of the arrows encode the sign of  $\langle \mathbf{S}_0 \cdot \mathbf{S}_i \rangle$  with arrows pointing northeast (southwest) indicating positive (negative) correlations. (c,d) The static spin structure factors corresponding to the states in (a,b), respectively. (e) The radially averaged nearest-neighbor correlator  $\mathcal{C}_a$  at  $\tilde{t}/t = 4$  for three width-4 cylinders of different lengths, showing the stripe-to-ferromagnet transition. Since the transition occurs between two different magnetically ordered symmetry-breaking states, by Landau theory, we expect it to be first-order, as borne out by the sudden jump in  $\mathcal{C}_a$ .

To study the stripe-ferromagnet quantum phase transition, we examine the correlator  $\mathcal{C}_a$ , which is plotted in Fig. 4(e) as a function of  $U/t$  for three different system sizes. The onset of ferromagnetism is apparent as a sharp increase in  $\mathcal{C}_a$  at  $U/t \sim 30$ , wherafter it quickly saturates to a system-size-independent value [53]. Intuitively, the order parameter remains pinned to this maximal value over an extended range of  $U/t$  because the gain of band energy due to a single flipped spin does not exceed the concomitant cost from the onsite repulsion; hence, we do

not observe a partially polarized ferromagnetic state.

*Discussion and outlook.*—Despite the prediction of Nagaoka ferromagnetism more than half a century ago, its actual realization has proved considerably more challenging. This may partially be attributed to the fragility of the Nagaoka state itself, which was theorized for an infinite system doped with exactly one hole at  $U/t = \infty$ . In this work, we address a central question: moving away from such an idealized limit, can ferromagnetism occur for finite  $U/t$  and macroscopic dopings? Using detailed DMRG computations, we reveal robust ferromagnetism (at least on moderate length scales), analyze its origins, and explore its intimate connections to the underlying lattice geometry. Given that half-filled Hubbard systems are generically either antiferromagnetic (when on a bipartite lattice) or paramagnetic, the emergence of ferromagnetism is indeed a beautiful demonstration of the surprises that strong correlations may engender.

The rarity of Nagaoka ferromagnetism in conventional solid-state materials is well documented. For instance, in many candidate Mott-insulator oxides and chalcogenide systems,  $U/t$  is insufficient to generate ferromagnetism. Likewise, strong positional disorder present in doped semiconductors often localizes mobile carriers and inhibits ferromagnetism [47, 54]. Optical lattice platforms, on the other hand, offer clean and tunable alternatives to circumvent these issues. In such systems, the lattice depth can be varied to control the tunnelings  $t, \tilde{t}$  while the ratio  $U/t$  can be tuned via a Feshbach resonance [55]. In the SM [40], we also discuss two possible methods to realize extended Hubbard models akin to Eq. (2), which could pave a new route to obtaining the Nagaoka state.

Even without any such correlated hoppings, our results for the case of  $\tilde{t} = t$  directly apply to the recent experiments of Ref. 30, which probe a square-lattice Hubbard model with a next-nearest-neighbor tunneling of strength  $t'$ . In the limit  $t \approx t'$  (when the square lattice is reconstructed to a triangular one), Xu *et al.* [30] observe signatures of ferromagnetic correlations for  $U/t \approx 9$  with  $\delta \approx 0.5$ . This is in excellent agreement with our predictions in Fig. 2, thus highlighting the geometric frustration of the kinetic energy as a mechanism for the experimentally observed ferromagnetism.

*Acknowledgments.*—We thank W.S. Bakr, M.L. Prichard, U. Schollwöck, E.M. Stoudenmire, and especially J. Kestner for useful discussions. R.S. is supported by the Princeton Quantum Initiative Fellowship. R.N.B. acknowledges support from the UK Foundation at Princeton University and thanks the Aspen Center for Physics, where some of the ideas were conceptualized, for hospitality. The simulations in this paper were performed using the ITENSOR library [56] on computational resources managed and supported by Princeton Research Computing, a consortium of groups including the Princeton Institute for Computational Science and Engineering (PICSciE) and the Office of Information Technology's

High Performance Computing Center and Visualization Laboratory at Princeton University.

*Note added.*—After the completion of this work, we became aware of two papers also studying Nagaoka ferromagnetism, which recently appeared on the arXiv [57, 58].

- 
- [1] D. P. Arovas, E. Berg, S. A. Kivelson, and S. Raghu, *Annu. Rev. Condens. Matter Phys.* **13**, 239 (2022).
  - [2] T. Schäfer, N. Wentzell, F. Šimkovic, Y.-Y. He, C. Hille, M. Klett, C. J. Eckhardt, B. Arzhang, V. Harkov, F.-M. Le Régent, A. Kirsch, Y. Wang, A. J. Kim, E. Kozik, E. A. Stepanov, A. Kauch, S. Andergassen, P. Hansmann, D. Rohe, Y. M. Vilch, J. P. F. LeBlanc, S. Zhang, A.-M. S. Tremblay, M. Ferrero, O. Parcollet, and A. Georges, *Phys. Rev. X* **11**, 011058 (2021).
  - [3] M. Qin, T. Schäfer, S. Andergassen, P. Corboz, and E. Gull, *Annu. Rev. Condens. Matter Phys.* **13**, 275 (2022).
  - [4] P. A. Lee, N. Nagaosa, and X.-G. Wen, *Rev. Mod. Phys.* **78**, 17 (2006).
  - [5] T. Esslinger, *Annu. Rev. Condens. Matter Phys.* **1**, 129 (2010).
  - [6] L. Tarruell and L. Sanchez-Palencia, *C. R. Phys.* **19**, 365 (2018).
  - [7] L. W. Cheuk, M. A. Nichols, K. R. Lawrence, M. Okan, H. Zhang, E. Khatami, N. Trivedi, T. Paiva, M. Rigol, and M. W. Zwierlein, *Science* **353**, 1260 (2016).
  - [8] M. F. Parsons, A. Mazurenko, C. S. Chiu, G. Ji, D. Greif, and M. Greiner, *Science* **353**, 1253 (2016).
  - [9] J. H. Drewes, L. A. Miller, E. Cocchi, C. F. Chan, N. Wurz, M. Gall, D. Pertot, F. Brennecke, and M. Köhl, *Phys. Rev. Lett.* **118**, 170401 (2017).
  - [10] A. Mazurenko, C. S. Chiu, G. Ji, M. F. Parsons, M. Kanász-Nagy, R. Schmidt, F. Grusdt, E. Demler, D. Greif, and M. Greiner, *Nature* **545**, 462 (2017).
  - [11] B. M. Spar, E. Guardado-Sanchez, S. Chi, Z. Z. Yan, and W. S. Bakr, *Phys. Rev. Lett.* **128**, 223202 (2022).
  - [12] E. Manousakis, *Rev. Mod. Phys.* **63**, 1 (1991).
  - [13] K. A. Chao, J. Spałek, and O. A. M., *Phys. Rev. B* **18**, 3453 (1978).
  - [14] P. W. Anderson, *Phys. Rev.* **115**, 2 (1959).
  - [15] Y. Nagaoka, *Phys. Rev.* **147**, 392 (1966).
  - [16] G.-s. Tian, *J. Phys. A: Math. Gen.* **23**, 2231 (1990).
  - [17] A. Sütő, *Commun. Math. Phys.* **140**, 43 (1991).
  - [18] T. Hanisch and E. Müller-Hartmann, *Ann. Phys. (Berl.)* **505**, 381 (1993).
  - [19] T. Hanisch, B. Kleine, A. Ritzl, and E. Müller-Hartmann, *Ann. Phys. (Berl.)* **507**, 303 (1995).
  - [20] P. Wurth, G. Uhrig, and E. Müller-Hartmann, *Ann. Phys. (Berl.)* **508**, 148 (1996).
  - [21] B. Douçot and X. G. Wen, *Phys. Rev. B* **40**, 2719 (1989).
  - [22] Y. Fang, A. E. Ruckenstein, E. Dagotto, and S. Schmitt-Rink, *Phys. Rev. B* **40**, 7406 (1989).
  - [23] B. S. Shastry, H. R. Krishnamurthy, and P. W. Anderson, *Phys. Rev. B* **41**, 2375 (1990).
  - [24] A. G. Basile and V. Elser, *Phys. Rev. B* **41**, 4842 (1990).
  - [25] A. Barbieri, J. A. Riera, and A. P. Young, *Phys. Rev. B* **41**, 11697 (1990).
  - [26] R. Strack and D. Vollhardt, *J. Low Temp. Phys.* **99**, 385

- (1995).
- [27] H. Tasaki, *Prog. Theor. Phys.* **99**, 489 (1998).
- [28] D. Vollhardt, N. Blümer, K. Held, M. Kollar, J. Schlipf, M. Ulmke, and J. Wahle, in *Advances in Solid State Physics 38* (Springer, 1999) pp. 383–396.
- [29] S. R. White, *Phys. Rev. Lett.* **69**, 2863 (1992); *Phys. Rev. B* **48**, 10345 (1993); U. Schollwöck, *Rev. Mod. Phys.* **77**, 259 (2005); *Ann. Phys.* **326**, 96 (2011).
- [30] M. Xu, L. H. Kendrick, A. Kale, Y. Gang, G. Ji, R. T. Scalettar, M. Lebrat, and M. Greiner, *Nature* **620**, 971 (2023).
- [31] D. C. Mattis, *The Theory of Magnetism I*, Springer Series in Solid-State Sciences (Springer Berlin, Heidelberg, 1981).
- [32] E. M. Stoudenmire and S. R. White, *Annu. Rev. Condens. Matter Phys.* **3**, 111 (2012).
- [33] J. Merino, B. J. Powell, and R. H. McKenzie, *Phys. Rev. B* **73**, 235107 (2006).
- [34] I. Morera, M. Kanász-Nagy, T. Smolenski, L. Ciorciaro, A. m. c. Imamoğlu, and E. Demler, *Phys. Rev. Res.* **5**, L022048 (2023).
- [35] J. Zaanen and O. Gunnarsson, *Phys. Rev. B* **40**, 7391 (1989).
- [36] K. Machida, *Physica C Supercond.* **158**, 192 (1989).
- [37] M. Kato, K. Machida, H. Nakanishi, and M. Fujita, *J. Phys. Soc. Jpn.* **59**, 1047 (1990).
- [38] J. M. Tranquada, B. J. Sternlieb, J. D. Axe, Y. Nakamura, and S.-i. Uchida, *Nature* **375**, 561 (1995).
- [39] M. Vojta, *Adv. Phys.* **58**, 699 (2009).
- [40] See Supplemental Material, which includes Refs. 59–69.
- [41] J. O. Haerter and B. S. Shastry, *Phys. Rev. Lett.* **95**, 087202 (2005).
- [42] W. Barford and J. H. Kim, *Phys. Rev. B* **43**, 559 (1991).
- [43] G. M. Pastor, R. Hirsch, and B. Mühlischlegel, *Phys. Rev. Lett.* **72**, 3879 (1994).
- [44] G. M. Pastor, R. Hirsch, and B. Mühlischlegel, *Phys. Rev. B* **53**, 10382 (1996).
- [45] T. Hanisch, G. S. Uhrig, and E. Müller-Hartmann, *Phys. Rev. B* **56**, 13960 (1997).
- [46] E. Nielsen and R. N. Bhatt, *Phys. Rev. B* **76**, 161202 (2007).
- [47] E. Nielsen and R. N. Bhatt, *Phys. Rev. B* **82**, 195117 (2010).
- [48] R. N. Bhatt and X. Wan, *Int. J. Mod. Phys. C* **10**, 1459 (1999); M. Berciu and R. N. Bhatt, *Phys. Rev. Lett.* **87**, 107203 (2001); R. N. Bhatt, M. Berciu, M. P. Kennett, and X. Wan, *J. Supercond.* **15**, 71 (2002).
- [49] A. Ghazali and P. L. Hugon, *Phys. Rev. Lett.* **41**, 1569 (1978).
- [50] N. F. Mott and J. H. Davies, *Philos. Mag. B* **42**, 845 (1980).
- [51] R. N. Bhatt and T. M. Rice, *Phys. Rev. B* **23**, 1920 (1981).
- [52] R. Samajdar and R. N. Bhatt, *Phys. Rev. B* **109**, 235128 (2024).
- [53] The collapse of the data for the two largest system sizes atop one another suggests that our observations are free of finite-size effects along the axial dimension.
- [54] R. N. Bhatt and P. A. Lee, *Phys. Rev. Lett.* **48**, 344 (1982).
- [55] C. Chin, R. Grimm, P. Julienne, and E. Tiesinga, *Rev. Mod. Phys.* **82**, 1225 (2010).
- [56] M. Fishman, S. R. White, and E. M. Stoudenmire, *SciPost Phys. Codebases*, 4 (2022).
- [57] C. Li, M.-G. He, C.-Y. Wang, and H. Zhai, (2023), [arXiv:2305.01682](https://arxiv.org/abs/2305.01682) [cond-mat.quant-gas].
- [58] H. Schlömer, U. Schollwöck, A. Bohrdt, and F. Grusdt, [arXiv:2305.02342](https://arxiv.org/abs/2305.02342) [cond-mat.str-el] (2023).
- [59] Y.-F. Jiang, J. Zaanen, T. P. Devereaux, and H.-C. Jiang, *Phys. Rev. Res.* **2**, 033073 (2020).
- [60] A. Wietek, Y.-Y. He, S. R. White, A. Georges, and E. M. Stoudenmire, *Phys. Rev. X* **11**, 031007 (2021).
- [61] D. Jaksch and P. Zoller, *Annals of physics* **315**, 52 (2005).
- [62] W. Hofstetter, J. I. Cirac, P. Zoller, E. Demler, and M. D. Lukin, *Phys. Rev. Lett.* **89**, 220407 (2002).
- [63] R. B. Diener and T.-L. Ho, *Phys. Rev. Lett.* **96**, 010402 (2006).
- [64] L.-M. Duan, *Phys. Rev. Lett.* **95**, 243202 (2005).
- [65] L.-M. Duan, *EPL* **81**, 20001 (2007).
- [66] J. P. Kestner and L.-M. Duan, *Phys. Rev. A* **81**, 043618 (2010).
- [67] J. P. Kestner and L. M. Duan, *New J. Phys.* **12**, 053016 (2010).
- [68] A. Rapp, X. Deng, and L. Santos, *Phys. Rev. Lett.* **109**, 203005 (2012).
- [69] M. D. Liberto, C. E. Creffield, G. I. Japaridze, and C. M. Smith, *Phys. Rev. A* **89**, 013624 (2014).

# Supplemental Material for “Nagaoka ferromagnetism in doped Hubbard models in optical lattices”

Rhine Samajdar<sup>1,2</sup> and R. N. Bhatt<sup>1,3</sup>

<sup>1</sup>*Department of Physics, Princeton University, Princeton, NJ 08544, USA*

<sup>2</sup>*Princeton Center for Theoretical Science, Princeton University, Princeton, NJ 08544, USA*

<sup>3</sup>*Department of Electrical and Computer Engineering,  
Princeton University, Princeton, NJ 08544, USA*

## SI. GROUND STATES ON WIDE CYLINDERS

In the main text, we showcased the magnetic ground states of both the regular and extended Hubbard models in different parameter regimes. These calculations were performed on long cylinders of varying length but with a fixed width of 4 sites. However, the results obtained on such strips may not necessarily be representative of an isotropic system in two dimensions. Accordingly, in this section, we scale the width in the transverse (periodic) direction to identify the properties that could survive in the fully two-dimensional model. Importantly, we demonstrate that the development of extended ferromagnetic ordering—observed earlier for the width-4 strips—holds even for the wider cylinders, thus allowing for the possibility that it does so in the true 2D limit as well.

### A. Triangular lattice

First, we study the simple Hubbard model

$$H_0 = -t \sum_{\langle i,j \rangle, \sigma} (c_{i\sigma}^\dagger c_{j\sigma} + \text{h.c.}) + U \sum_i n_{i\uparrow} n_{i\downarrow}, \quad (\text{S1})$$

on a triangular lattice embedded on a width-6 cylinder, where  $n_{i,\sigma} \equiv c_{i,\sigma}^\dagger c_{i,\sigma}$  denotes the number operator on site  $i$ , and  $n_i = n_{i,\uparrow} + n_{i,\downarrow}$  is the total occupation of site  $i$ . Here, we set the electron doping concentration to  $\delta = 0.5$ , as before, and focus on a lattice of dimensions  $12 \times 6$  which maintains the same aspect ratio as the  $8 \times 4$  cylinder studied in the main text. This wider geometry provides additional insights into the emergence and stability of the ferromagnetic phase as the 2D limit is approached.

Our results, displayed in Fig. S1, are qualitatively similar to those for the width-4 cylinder studied in the main text. At low  $U/t=6$ , the ground state exhibits stripe (unidirectional) ordering in the spin sector, as evidenced by the spin-spin correlations plotted in Fig. S1(a), while the charge density is approximately uniform. This spontaneous development of spin-density-wave order occurs due to the competition between the antiferromagnetic superexchange—which favors domain walls in the spin texture—and the energetic cost of dopant electrons being localized to each stripe, with the former prevailing. On increasing  $U/t$  further, the period of the stripes increases [as seen in Fig. S1(b)] as the polarized domains

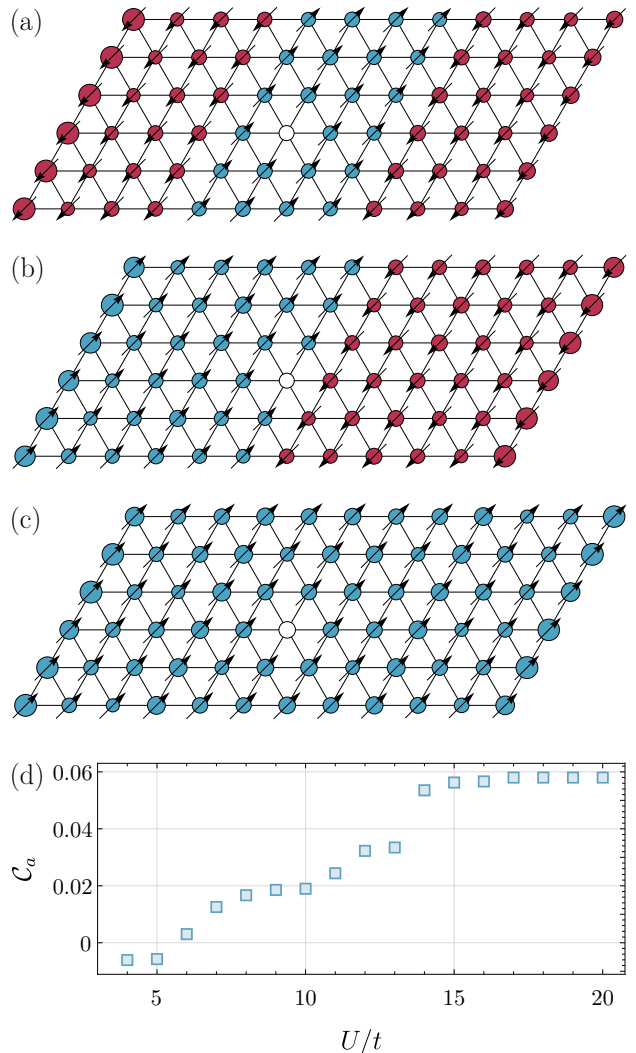


Figure S1. Ground states of the Hubbard model, with cylindrical boundary conditions, on a  $12 \times 6$  triangular lattice doped with 36 electrons, for (a)  $U/t=6$ , (b)  $U/t=12$ , and (c)  $U/t=16$ . The diameter of the circles is scaled according to the local excess electron density  $\langle n_i \rangle - 1$ . The length of the arrow on each site is proportional to the magnitude of  $\langle \mathbf{S}_0 \cdot \mathbf{S}_i \rangle$ , with the central (white, unmarked) site selected as the reference spin  $\mathbf{S}_0$ . The orientation of the arrow and the color of the circle on each site indicates the sign of the spin correlations, with blue (red) denoting positive (negative) correlations. (d) The average nearest-neighbor correlation, plotted as a function of  $U/t$ , saturates to its maximum possible value in the fully polarized ferromagnetic phase.

partially merge and expand. This reorganization is driven the kinetic energy gain from delocalization over a larger domain as compared to the weakened exchange interaction at larger  $U/t$ . Finally, around  $U/t \sim 14$ , the kinetic term wins outright and the system transitions to the fully polarized ferromagnetic state, as exemplified by Fig. S1(c).

This behavior is reflected in the normalized averaged two-point correlation function  $\mathcal{C}_a = \sum_{\langle i,j \rangle, \|\mathbf{r}_i - \mathbf{r}_j\|=a} \langle \mathbf{S}_i \cdot \mathbf{S}_j \rangle / (2N)$ , where the sum runs over unordered pairs of nearest-neighbor sites  $\langle i,j \rangle$  separated by the lattice spacing  $a$ . Figure S1(d) shows that  $\mathcal{C}_a$  starts off at a positive value in the striped phase (indicating the presence of local ferromagnetic correlations as expected from the stripe ordering) before eventually saturating to its maximal value for the global ferromagnet at larger  $U/t$ . Note that the critical value of  $U/t$  required to obtain the Nagaoka state still remains much less than that needed on the square lattice due to the kinetic origin of the ferromagnetism.

A cylinder with a circumference of 6 sites is close to the current limit of state-of-the-art ground-state DMRG numerics [1, 2] and it is presently challenging, if not unfeasible, to obtain fully converged results using DMRG for wider strips. However, the fact that our results on the 2-leg ladder as well as the 4-, and 6-site-wide cylinders are broadly consistent suggests that a fully spin-polarized ferromagnetic ground state may exist for much larger widths, at finite dopings and sufficiently large  $U/t$ , and possibly in the 2D thermodynamic limit as well.

## B. Square lattice

On the square lattice, we consider the extended Hubbard model defined by the Hamiltonian

$$H = - \sum_{\langle i,j \rangle, \sigma} \left( t(n_i, n_j) c_{i\sigma}^\dagger c_{j\sigma} + \text{h.c.} \right) + U \sum_i n_{i\uparrow} n_{i\downarrow}, \quad (\text{S2})$$

where the occupation-dependent nearest-neighbor hopping is given by

$$t(n_i, n_j) = \begin{cases} \tilde{t}, & \text{if } n_i = 1, n_j = 2 \\ t, & \text{if } n_i = 0, n_j = 2 \\ t, & \text{if } n_i = 1, n_j = 1 \\ t, & \text{if } n_i = 0, n_j = 1 \\ 0, & \text{otherwise} \end{cases} \quad (\text{S3})$$

As discussed in the main text, the enhanced hopping amplitude of the loosely bound second electron on any given site helps facilitate ferromagnetism which would otherwise require prohibitively large values of  $U/t$  for the square lattice. Here, we extend our calculations to cylinders with widths of 5 and 6 sites, while keeping  $\tilde{t}/t = 4$  and a doping fraction of  $\delta = 1/12$  as before.

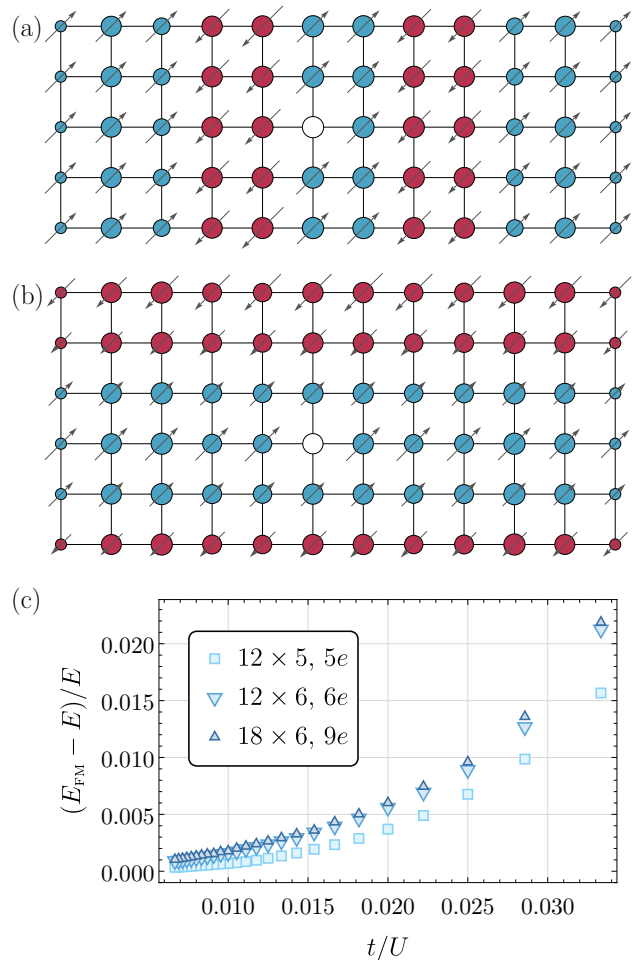


Figure S2. Ground states, with cylindrical boundary conditions, on a (a)  $12 \times 5$ , and (b)  $12 \times 6$  square lattice doped with an excess electron density of  $\delta = 1/12$  for  $\tilde{t}/t = 4$ ,  $U = 10\tilde{t}$ . The charge densities and spin-spin correlations are plotted using the same conventions as in Fig. S2. (c) Difference between the numerically obtained energies for the Nagaoka ferromagnetic state,  $E_{\text{FM}}$  and the true ground state yielded by DMRG,  $E$ , as a function of  $(U/t)^{-1}$ .

Firstly, on a  $12 \times 5$  cylinder doped with 5 electrons, we observe the emergence of stripe ordering at moderately large values of  $U/t$ , with the spin density modulated along the length of the cylinder. Thus, the system forms extended domains with ferromagnetic order [Fig. S2(a)], which is consistent with our numerics on width-4 cylinders. However, in contrast to the situation for narrower strips, we find that global ferromagnetism remains absent for up to at least  $U/t = 150$ . This difference can be attributed to the fact that for a fixed  $L_x$  and  $\delta$ , the superexchange energy from the domain walls—and correspondingly, the critical strength of  $U/t$  required to fully polarize the system—grows as  $L_y^2$ , assuming unit-filled stripes. Nevertheless, as one increases  $U/t$ , the ferromagnetic domains enlarge further; e.g., for  $U/t \sim 100$ , the ground state hosts three stripes, with two of length 5

starting from either end of the cylinder and a third one of length 2 between them.

Interestingly, on the width-6 cylinders (either 12- or 18-site-long), we once again observe stripe orders, but now with two stripes running parallel to the cylinder's length, i.e., the modulation of the spin density is *perpendicular* to the axial direction. Such a configuration allows for a long exchange-favored domain wall while the cylinder's relatively large width optimizes the associated kinetic cost by ensuring that the doublons are delocalized over an extended area (had the stripes been oriented otherwise, each dopant would be confined to a much narrower domain). This longitudinal stripe phase persists as the ground state for up to very large values of  $U/t$  (we find that till at least  $U/t = 150$ , it is resistant to global ferromagnetic ordering). This conclusion is also insensitive to the length of the cylinder and applies to both the  $12 \times 6$  and  $18 \times 6$  systems.

In order to probe this behavior systematically, in Fig. S2(c), we plot the relative difference between the energies of the ideal fully polarized Nagaoka ferromagnet ( $E_{\text{FM}}$ ) and the actual ground state, determined using DMRG ( $E$ ) as a function of  $(U/t)^{-1}$ . This quantity decreases as  $t/U \rightarrow 0$  but remains positive throughout our numerically studied range of  $U/t$  (down to  $t/U = 1/150$ ), signaling the lack of global ferromagnetic order. By examining the polynomial fits of the energy differences, we ascertain that there always exists a real root of  $E_{\text{FM}} - E = 0$  for some  $t/U > 0$  on the width-3, -4, -5, and -6 cylinders. This is suggestive of and consistent with a scenario in which for any *finite* doped 2D system, global Nagaoka ferromagnetism occurs at a finite, albeit large,  $U/t < \infty$  whereas extended ferromagnetically ordered domains on the nanoscale can be attained for orders-of-magnitude lower  $U/t$ .

## SII. REALIZATION OF GENERALIZED HUBBARD MODELS

The extended Hubbard model that we have analyzed in this work was originally introduced to study hydrogenic donors in semiconductors [3, 4; see also 5–7]. In such a solid-state setting, the hopping parameter is naturally occupation-dependent due to the nearly twentyfold difference in the binding energies of the one-electron  $1s$  bound state and the two-electron state ( $\text{H}^-$ ). On the contrary, a weakly interacting gas in an optical lattice is well-described by simply the one-band Hubbard model [8, 9].

In the following, we bridge this gap and discuss two proposals for realizing models similar to Eq. (S2) in optical lattice platforms.

### A. Lattice anharmonicity-induced resonances

For a gas of interacting ultracold fermionic atoms near a Feshbach resonance, the conventional derivation of a single-band Hubbard model [8, 9] does not hold because the onsite interaction energy exceeds the lattice bandgap [10]. Nonetheless, Duan [11, 12] showed that even this strongly interacting regime can be captured by an effective single-band lattice Hamiltonian corresponding to a *generalized* Hubbard model. This is due to an emergent restriction on the effective Hilbert space dimension: even though a state with two atoms on one site populates multiple lattice bands, only one two-atom eigenlevel—termed a “dressed molecule”—is relevant while the others can be adiabatically eliminated due to a large energy splitting. Thus, each site can only be empty or populated with either one atom or a dressed molecule with a fixed internal state. In general, for a fixed chemical potential, the effective Hamiltonian is given by [11, 12]

$$\mathcal{H} = U \sum_i n_{i\uparrow} n_{i\downarrow} - t_d \sum_{\langle i,j \rangle \sigma} c_{i\sigma}^\dagger c_{i\bar{\sigma}}^\dagger c_{j\bar{\sigma}} c_{j\sigma} \quad (\text{S4})$$

$$- \sum_{\langle i,j \rangle \sigma} \left[ t + (g - t)(n_{i\bar{\sigma}} + n_{j\bar{\sigma}}) + (\tilde{t} + t - 2g) n_{i\bar{\sigma}} n_{j\bar{\sigma}} \right] c_{i\sigma}^\dagger c_{j\sigma}.$$

Here,  $g$  is the particle-assisted tunneling rate,  $\tilde{t}$  is the rate for an atom to hop from a doubly occupied site to a singly occupied one, and  $t_d$  is the dimer (or molecular) tunneling rate. Note that  $\mathcal{H}$  can be recast into the form

$$\mathcal{H} = - \sum_{\langle i,j \rangle, \sigma} \left( t(n_i, n_j) c_{i\sigma}^\dagger c_{j\sigma} + \text{h.c.} \right) + U \sum_i n_{i\uparrow} n_{i\downarrow},$$

where

$$t(n_i, n_j) = \begin{cases} \tilde{t}, & \text{if } n_i = 1, n_j = 2 \\ g, & \text{if } n_i = 0, n_j = 2 \\ g, & \text{if } n_i = 1, n_j = 1 \\ t, & \text{if } n_i = 0, n_j = 1 \end{cases}, \quad (\text{S5})$$

which reduces to Eq. (S2) if  $g = t \neq \tilde{t}$ .

The parameters of this effective Hamiltonian were computed by Ref. 13, which studies the energy spectrum of two indistinguishable fermions interacting in a lattice (as characterized by an  $s$ -wave scattering length,  $a_s$ ) in an external potential  $V(\mathbf{r})$  given by the sum of a periodic part,  $V_0 \prod_{i=1}^3 \cos^2 k_L r_i$ , and a harmonic confining potential. The two-atom, double-well physics can be approximated with a generalized Hubbard model only if there is a separation of energy scales such that a well-isolated manifold of four energy levels exists. This condition is satisfied far from unitarity (i.e.,  $k_L a_s = 0$ ) on either side [13]. Moreover, right at and around unitarity, there is another narrow window for which an effective one-band general Hubbard model applies. Importantly, this arises due to a lattice-induced anharmonic coupling between

atoms at the scattering threshold and a weakly bound Feshbach molecule in an excited center-of-mass state [14].

By a similar argument, it is reasonable to expect that the parameter  $\tilde{t}$  might become significantly larger than  $t$  and  $g$  in a very narrow region where a deeply bound dimer with a large center-of-mass kinetic energy goes through an anharmonicity-mediated avoided crossing with the unbound atomic pair in the lowest band [15]. Near an anharmonicity-induced resonance  $(g-t)/t < 0.2$  for both positive and negative values of  $-1/(k_L a_s)$ , so the generalized Hubbard model studied in the main text is a good approximation. While operating in this regime also induces a non-negligible  $t_d$  (which can be  $\mathcal{O}(1)$  for  $-1/(k_L a_s) < 0$ ), this is irrelevant to the problem at hand because we focus on dopings above half filling, wherefore dimer-hopping processes are strongly suppressed.

## B. Floquet driving

Another potential route for the implementation of Hubbard models with correlated hopping processes, such as in Eq. (S2), is to start off with a system of fermions in the lowest band of an optical lattice and to periodically modulate the interactions in time by using a Feshbach resonance [16]. The time-dependent Hamiltonian reads

$$\mathcal{H}_F = -h \sum_{\langle i,j \rangle, \sigma} \left( c_{i\sigma}^\dagger c_{j\sigma} + \text{h.c.} \right) + \mathcal{U}(t) \sum_i n_{i\uparrow} n_{i\downarrow}, \quad (\text{S6})$$

where  $\mathcal{U}(t) \equiv U_0 + U_1 \cos(\omega t)$ . Note that, here, we use  $h$  to denote the hopping matrix element to avoid any notational ambiguity since the interaction explicitly depends on the time  $t$ . However, in the high-frequency regime  $\omega \gg h, U_0$ , the time-independent Floquet Hamiltonian is approximated by an effective static Hamiltonian given by [17]

$$\begin{aligned} \mathcal{H}_{\text{eff}} = & -h \sum_{\langle i,j \rangle, \sigma} \left( c_{i\sigma}^\dagger c_{j\sigma} + \text{h.c.} \right) \mathcal{J}_0 \left[ \chi (n_{i\bar{\sigma}} - n_{j\bar{\sigma}}) \right] \\ & + U_0 \sum_i n_{i\uparrow} n_{i\downarrow}, \end{aligned} \quad (\text{S7})$$

with  $\mathcal{J}_0$  denoting a Bessel function of the first kind and  $\chi \equiv U_1/\omega$ . Expanding the Bessel function as a Taylor series (which only has even terms), and using the fermion identity  $(n_{i\sigma} - n_{j\sigma})^{2p} = n_{i\sigma} + n_{j\sigma} - 2n_{i\sigma}n_{j\sigma} \forall p > 0$ , we arrive at [17]

$$\mathcal{H}_{\text{eff}} = -h \sum_{\langle i,j \rangle, \sigma} \left( c_{i\sigma}^\dagger c_{j\sigma} + \text{h.c.} \right) + U_0 \sum_i n_{i\uparrow} n_{i\downarrow} \quad (\text{S8})$$

$$+ h \sum_{\langle i,j \rangle, \sigma} \left( c_{i\sigma}^\dagger c_{j\sigma} + \text{h.c.} \right) \left[ \tilde{\chi} (n_{i\bar{\sigma}} + n_{j\bar{\sigma}} - 2n_{i\bar{\sigma}}n_{j\bar{\sigma}}) \right],$$

where we have introduced  $\tilde{\chi} \equiv 1 - \mathcal{J}_0(\chi)$ .

Written in the language of Eq. (S2), this defines a Hubbard model with an occupation-dependent hopping specified as

$$h(n_i, n_j) = \begin{cases} h, & \text{if } n_i = 1, n_j = 2 \\ h \mathcal{J}_0(\chi), & \text{if } n_i = 0, n_j = 2 \\ h \mathcal{J}_0(\chi), & \text{if } n_i = 1, n_j = 1 \\ h, & \text{if } n_i = 0, n_j = 1 \end{cases}. \quad (\text{S9})$$

Now, by tuning the strength and frequency of the external driving such that  $\chi$  is close to 2.4048... (the first zero of the Bessel function), one can render  $\mathcal{J}_0(\chi)$ —and consequently, the two hoppings on the second and third lines above—arbitrarily small relative to the bare hopping  $h$ . These hopping processes are precisely the ones responsible for the spin superexchange, so in this mechanism, we promote ferromagnetism by weakening the exchange.

Alternatively, it is straightforward to see that Eq. (S8) can be rewritten as  $\mathcal{H}_{\text{eff}} =$

$$\mathcal{J}_0(\chi) \left[ - \sum_{\langle i,j \rangle, \sigma} \left( t(n_i, n_j) c_{i\sigma}^\dagger c_{j\sigma} + \text{h.c.} \right) + U \sum_i n_{i\uparrow} n_{i\downarrow} \right],$$

which is simply a rescaled version of the extended Hubbard model in Eq. (S2) with  $U \equiv U_0/\mathcal{J}_0(\chi)$  and

$$t(n_i, n_j) = \begin{cases} h/\mathcal{J}_0(\chi), & \text{if } n_i = 1, n_j = 2 \\ h, & \text{if } n_i = 0, n_j = 2 \\ h, & \text{if } n_i = 1, n_j = 1 \\ h/\mathcal{J}_0(\chi), & \text{if } n_i = 0, n_j = 1 \end{cases}. \quad (\text{S10})$$

Thus, the hopping from a doubly occupied site to a singly occupied one is increased by a factor of  $1/\mathcal{J}_0(\chi)$ , which, as mentioned above, can be tuned to be  $\gg 1$ . Moreover, we see that the resultant  $U$  is obtained from an enhancement of the bare  $U_0$  by the same factor, and therefore one can attain values of  $U/h \gg 1$  even if  $U_0/h \sim \mathcal{O}(1)$  (which ensures that we have a proper single-band lattice description to begin with). Finally, note that while the hopping from a singly occupied lattice site to an empty site is also enhanced, such processes are suppressed since we are always considering electron dopings (above half filling)—hence, we expect to observe the same physics as the model in Eq. (S2) using this Floquet scheme.

- 
- [1] Y.-F. Jiang, J. Zaanen, T. P. Devereaux, and H.-C. Jiang, *Phys. Rev. Res.* **2**, 033073 (2020).  
[2] A. Wietek, Y.-Y. He, S. R. White, A. Georges, and E. M.

- Stoudenmire, *Phys. Rev. X* **11**, 031007 (2021).  
[3] E. Nielsen and R. N. Bhatt, *Phys. Rev. B* **76**, 161202 (2007).

- [4] E. Nielsen and R. N. Bhatt, *Phys. Rev. B* **82**, 195117 (2010).
- [5] R. N. Bhatt and X. Wan, *Int. J. Mod. Phys. C* **10**, 1459 (1999).
- [6] M. Berciu and R. N. Bhatt, *Phys. Rev. Lett.* **87**, 107203 (2001).
- [7] R. N. Bhatt, M. Berciu, M. P. Kennett, and X. Wan, *J. Supercond.* **15**, 71 (2002).
- [8] D. Jaksch and P. Zoller, *Annals of physics* **315**, 52 (2005).
- [9] W. Hofstetter, J. I. Cirac, P. Zoller, E. Demler, and M. D. Lukin, *Phys. Rev. Lett.* **89**, 220407 (2002).
- [10] R. B. Diener and T.-L. Ho, *Phys. Rev. Lett.* **96**, 010402 (2006).
- [11] L.-M. Duan, *Phys. Rev. Lett.* **95**, 243202 (2005).
- [12] L.-M. Duan, *EPL* **81**, 20001 (2007).
- [13] J. P. Kestner and L.-M. Duan, *Phys. Rev. A* **81**, 043618 (2010).
- [14] J. P. Kestner and L. M. Duan, *New J. Phys.* **12**, 053016 (2010).
- [15] J. P. Kestner, Private communication.
- [16] A. Rapp, X. Deng, and L. Santos, *Phys. Rev. Lett.* **109**, 203005 (2012).
- [17] M. D. Liberto, C. E. Creffield, G. I. Japaridze, and C. M. Smith, *Phys. Rev. A* **89**, 013624 (2014).